FACTA UNIVERSITATIS (NIŠ)
SERIES: ELECTRONICS AND ENERGETICS VOL. 7, NO. 1 (1994), 83-90

COMPUTER GENERATION OF THERMAL IMAGES AND ANALYSIS OF LINE–SCANNING EFFECTS

Aleksandar Marinčić, Žarko Barbarić, Grozdan Petrović and Dragorad Milovanović

Abstract. A computer model for the generation of thermal images of a quasi-natural terrain by line-scanning technique from a moving platform is presented. Several computer generated thermal images are produced to illustrate the model. The geometrical deformations, space filtration, gray level variation and change of statistical parameters with the scanning angle for generated images are in agreement with theoretical predictions. The analysis of statistical parameters of computer generated thermal images by line-scanning technique indicate approach to efficient image transmission.

Key words: Thermal image, line scanning effects, statistical analysis, video signal.

1. Introduction

Thermal infrared image is produced by the distribution of the radiant exitance of a scene transformed through an optomechanical scanning device into a flux incident on the detector. The video signal at the detector output is proportional to the incident flux from the terrain and the atmosphere, within a specified wavelength range. This range is selected on the basis that the average temperature of the natural terrain is between 250 and 350 K, which means that the peak radiation is in the range from 11.6 to 8.3 μm, respectively. At the same time this wavelength range is convenient because of the high atmospheric spectral transmittance and good spectral response of detectors.

Manuscript received February 8, 1993.
The authors are with Faculty of Electrical Engineering, University of Belgrade, 11000 Belgrade.

In reality generation of an infrared thermal image is a complex process not easily modeled in a general case. A simulation model SENSAT-2 (Sensor-Atmosphere-Target) is presented by Richter [1]. This model was developed for remote sensing applications of passive sensors in the infrared spectral region 1-28μm. The natural terrain modeling has been suggested by Ben-Yosef et al [2]. A method for simulating sea surface images obtained by forward-looking infrared (FLIR) sensors in the 8-12 μm band presented by Wilf and Manor [3]. A new computer model for generation of thermal images by line-scanning technique is developed by Barbaric et al [4], in the spectral range 8-14 μm.

2. Simulation model

Simulation model used in this paper is based on the theory given in our earlier model [4]. A schematic diagram of this model is shown in Fig.1. The model consists of terrain, atmosphere and line scanner. The terrain is simulated as a periodic repetition of the terrain base area, made from ground and objects base areas. The terrain base area is formed as a combination of ground between the objects. The objects in the terrain base area are defined by their non–overlapping contours. Statistical parameters for ground and each object such as the mean temperature distributions, the standard deviations and the correlation lengths are specified.

Based on the specified parameters for each object and ground areas we generate by a pseudorandom generator (PRG) the two–dimensional Gaussian temperature distribution $T(i,k),\ i = 0, 1, 2, \dots, (N-1)$. As thus obtained temperature distributions are not spatially correlated, we correct these by taking into account the spatial autocorrelation function (ACF), in the spatial frequency domain using the discrete Fourier transform (DFT). The correlated temperature distribution is obtained as the inverse discrete Fourier transform (IDFT). In this way we calculate the discrete temperature distribution of the ground area $T_C^G(i,k)$ and the object areas $T_C^O(i,k)$. The temperature distribution of the terrain base area $T_C^T(i,k)$ is obtained as the union of the above specified temperature distributions. The terrain radiance is calculated from $T_C^T(i,k)$ as shown in Fig.1 based on ref [4].

The atmospheric radiance $L_C^A(i,k)$ is calculated in an analogous way to the terrain radiance. The transmittance τ, of atmosphere is a function of scanning angle Θ and the average transmittance $\overline{\tau}$ at the nadir. We assumed that $\tau = \tau^{sec\Theta}$. The optomechanical scanner can be interpreted as a device which collects radiance flux from elementary areas within resolution cell and the atmosphere volume within the sensor cone solid angle.

The voltage at the detector output is obtained in the form a double sum [4]

$$V(i,k) = \sum_{m=0}^{M-1} \sum_{n=0}^{N-1} K_1 \big[\tau L_C^T(m,n) + L_C^A(m,n)\big] H(m,n,\Theta_k) \exp\big[2\pi j(\frac{m}{M}i + \frac{n}{N}k)\big]$$

where $K_1 = A_0 k_0 R \alpha_0 \beta_0$ is a constant, $i = 0,1,2,\dots$ and $k = 0,1,2,\dots$. The numbers M and N are selected so that all available samples of radiance over the terrain base area are included. The radiances $L_C^T(m,n)$ and $L_C^A(m,n)$ are the discrete Fourier transform of the terrain radiance $L_C^T(i,k)$, and the atmosphere radiance $L_C^A(i,k)$. The normalized optical transfer function is $H(m,n,\Theta_k)$ where $\Theta_k = \arctan(k\Delta y/H)$ and H is the altitude of platform. In the calculation of $H(m,n,\Theta_k)$ Hermitian symmetry with respect to m and n is taken into account.

The output signal from the detector has to be resampled and quantized. The quantized gray level of infrared thermal image is obtained through a processing operation on the resampled voltage $V(i,k)$, as shown in Fig. 1.

3. Generated thermal images and analysis of line-scanning effects

Using the developed computer model a number of thermal images were generated and the effects of line scanning, spatial resolution and some statistical image parameters were studied.

A representative example of the computer–generated image of a terrain base area with four square hot–plates on the ground is shown in Fig. 2a, for a selected set of statistical parameters.

The terrain base area was periodically extended along the x– and y– axes. This terrain was scanned with the line scanning parameters: $\alpha_0 = \beta_0 = 1.5 mrad$, $\Delta X = H\alpha_0 = 1m$ and $\Delta\Theta = \beta_0$.

In practice, we select a limited number of pixels p and q and from a frame of thermal image. The frame covers the scanning angles from Θ_0 to $\Theta_0 + q\Delta\Theta$, where Θ_0 is an arbitrarily selected angle measured from the nadir. Figs.2b to 2g show two computer generated frames corresponding to the scanning angle ranges: $\Theta^\circ < \Theta < 5.5^\circ$ and $60^\circ < \Theta < 65.5^\circ$, for different ratios of mean atmosphere to ground temperature. These frames are parts of the terrain thermal image. The dimensions of each frame are

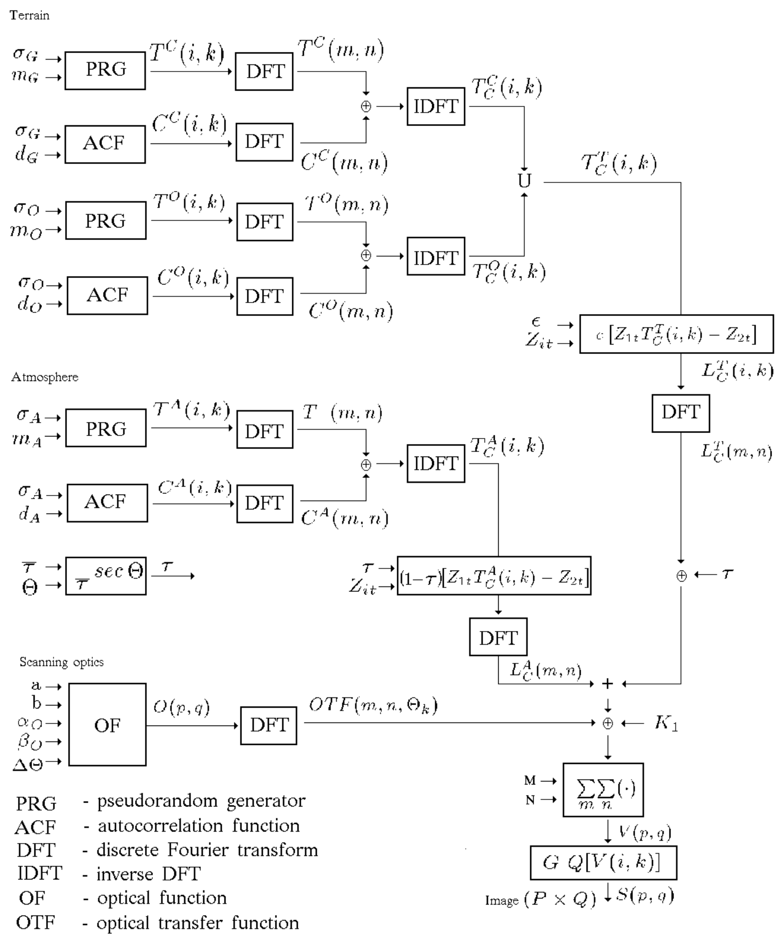

Fig. 1.

64×64 pixels. The image frames were generated with 256 gray levels, but the image frames shown in this paper are printed with 26 gray levels (hot is black).

The difference between Fig. 2b and the corresponding part of Fig. 2a is almost negligible because the line scanning effects are small close to the nadir. The geometrical effects of line scanning are clearly seen in Fig. 2c. They are manifested as the blurred edges and the change in the sizes of the plates. Another effect of the line scanning is the change of the gray level

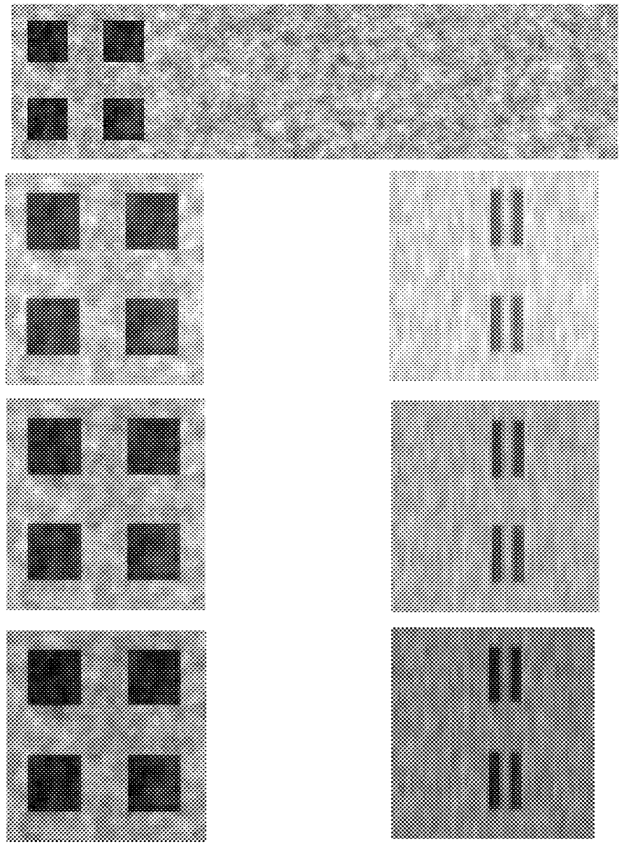

Fig. 2. *Frames of computer generated terrain thermal image for different ratios of atmosphere to ground average temperature* m_A/m_G*:*

(a) Computer generated the terrain base area of dimensions 64 m× 256 m, plates of dimensions 16 m×16 m (shown scaled down in comparison with other frames). Parameters are: $m_G = 289$ *K,* $\sigma_G = 1.25$ *K,* $d_G = 2m$*,* $m_p = 306$ *K,* $\sigma_p = 1K$*,* $d_p = 4$ *m,* $\varepsilon = 0.9$*.*

(b) The scanned part of terrain base area for m_A/m_G*=290 K/298 K and* $0° < \Theta < 5.5°$*;*

(c) The scanned terrain base area for m_A/m_G*=290 K/298 K and* $60° < \Theta < 65.5°$*;*

(d) The scanned part of terrain base area for m_A/m_G*=298 K/298 K and* $0° < \Theta < 5.5°$*;*

(e) The scanned terrain base area for m_A/m_G*=290 K/298 K and* $60° < \Theta < 65.5°$*;*

(f) The scanned part of terrain base area for m_A/m_G*=306 K/298 K quad and* $0° < \Theta < 5.5°$*;*

(g) The scanned terrain base area for m_A/m_G*=306 K/29 8K and* $60° < \Theta < 65.5°$*;*

fluctuation with the scanning angle.

To illustrate the effects of atmosphere radiation and attenuation the three characteristic cases for different ratios of average atmosphere to ground temperature are shown in Fig. 2b–2g. In all cases the average atmosphere transmittance was constant ($\tau = 0.85$). The frames shown in Fig. 2b and 2c are typical for a sunny day, when $m_A/m_G < 1$ Fig.2d and 2e are for $m_A/m_G = 1$, and Fig.2f and 2g are typical for a night, when $m_A/m_G > 1$. As can be seen from these figures the average gray level and the image contrast change with the ratio m_A/m_G, indicating variation in the thermal image quality during day and night, which is in agreement with the investigated by Ben–Yosef et al [5].

Statistical parameters [6] of thermal images of different type of terrain are analyzed in order to study the possibility of efficient transmission of digitized images.

The statistical parameters of computer generated thermal image shown partially in Fig.2 are calculated for five frames and then analyzed. The selected frames correspond to the scanning angle ranges: $0° < \Theta < 5.5°$, $15° < \Theta < 20.5°$, $30° < \Theta < 35.5°$, $40° < \Theta < 45.5°$ and $55° < \Theta < 60.5°$.

The mean value as a function of the scanning angle is shown in Fig. 3a. The ground mean temperature is assumed higher then the atmosphere mean temperature ($m_A > m_G$) and the mean value gray level in this case decreases with the scanning angle, for $m_A = m_G$ the mean value is constant, and in case $m_A < m_G$ the mean value increases with the scanning angle.

In Fig. 3b the standard deviation of gray level as a function of the scanning angle is shown. The standard deviation decreases with the scanning angle because of increasing area of the projected instantaneous field of view of the scanning optics (the resolution cell). Changes of standard deviation with the scanning angle can be used in selection of an optimal quantization of thermal image signal samples as the function of scanning angle.

Fig. 3c shows results for the two autocorrelation coefficients for neighboring pixels. In the along track direction the autocorrelation coefficient (R_1^1) increases with the scanning angle because in this case we have increased overlapping of the neighboring scanning terrain tracks. The across–track direction correlation coefficient (R_2^1) decreases because the distance between centers of the neighboring resolution cells increase with the scanning angle. It should be noticed that in spite of the assumption that the terrain is assumed isotropic, the correlation of the thermal image formed by the line scanning is unisotropic. The change of correlation coefficients can be used

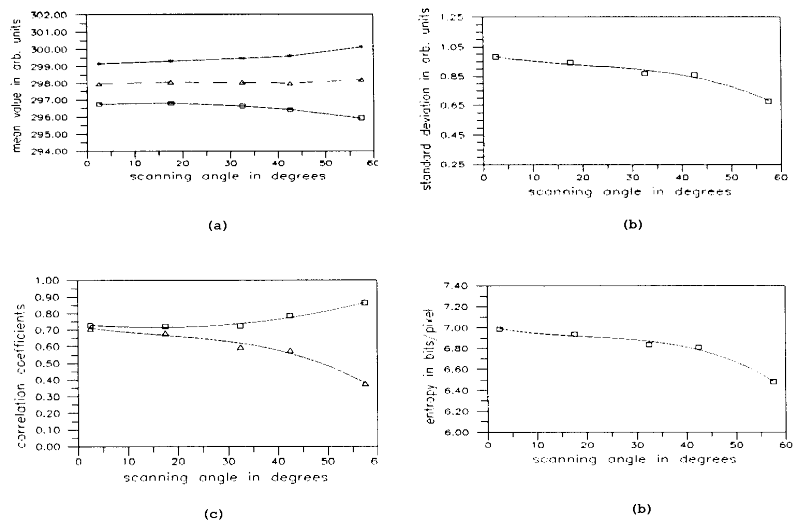

Fig. 3. The variation of mean value (a), standard deviation (b), autocorrelation coefficients (c) and entropy (d) with scanning angle.

in selection of the weighting coefficients in the predictive coding.

Fig. 2d shows change of entropy of the generated thermal image as a function of scanning angle. The entropy decreases with the scanning angle because of decrease of gray level standard deviation. The change of entropy with the scanning angle proves that a statistical coding with a variable word length can be used.

All the above statements are based on computer generated thermal image of typically correlated terrain, but in view of the available experimental results, it is expected that the same conclusions are valid for real thermal images produced by the line scanning technique.

4. Conclusion

Several computer generated thermal images illustrate the line scanning distortion, the change of the gray level fluctuation, and the change of mean gray level for various atmosphere to terrain temperature ratios.

From the analysis of statistical parameters of computer generated thermal images of typically correlated terrain, we found that there are changes of the parameters that can be advantageously used for the redundancy reduction and selection of predictive and statistical coding. The efficiency of proposed techniques for data compression depends on the type of terrain and require further study in order to arrive at an optimal solutions.

REFERENCES

1. R. Richter: *Infrared Simulations Model SENSAT–2.* DFVLR–FB 87–10, Institut fur Optoelektronik, Oberpfaffenhofen (1987)
2. N. Ben–Yosef, K. Wilner and M. Abitbol: *Measurement and Modeling of Natural Desert Terrain in the Infrared.* Optical Engineering, Vol.27 No.11. 928–932 (1988)
3. I. Wilf and Y. Manor: *Simulation of Sea Surface in the Infrared.* Applied Optics, Vol.23 No.18, 3174–3180 (1984)
4. Z. Barbarić, a> Marinčić, G. Petrović, D. Milovanović: *A New Computer Model for Generation of Thermal Images by Line–scanning Technique.* Accepted to publication in Applied Optics, 1993
5. N. Ben–Yosef, S. Lashansky, K. Wilner and M. Abitbol: *Temporal Prediction of Infrared Images of Ground Terrain.* Applied Optics, Vol.26 No.11,2128–2130 (1987)
6. Z. Barbarić, A. Marinčić, G. Petrović, D. Milovanović: *Statistical Properties of Thermal Images Generated by Line–scanning Technique.* Accepted to publication in Applied Optics, 1994